ANTHROPOLOGY

Morphology of the Denisovan phalanx closer to modern humans than to Neanderthals

E. Andrew Bennett[1]*†, Isabelle Crevecoeur[2]*†, Bence Viola[3,4]*†, Anatoly P. Derevianko[4,5], Michael V. Shunkov[4,6], Thierry Grange[1], Bruno Maureille[2], Eva-Maria Geigl[1]†

A fully sequenced high-quality genome has revealed in 2010 the existence of a human population in Asia, the Denisovans, related to and contemporaneous with Neanderthals. Only five skeletal remains are known from Denisovans, mostly molars; the proximal fragment of a fifth finger phalanx used to generate the genome, however, was too incomplete to yield useful morphological information. Here, we demonstrate through ancient DNA analysis that a distal fragment of a fifth finger phalanx from the Denisova Cave is the larger, missing part of this phalanx. Our morphometric analysis shows that its dimensions and shape are within the variability of *Homo sapiens* and distinct from the Neanderthal fifth finger phalanges. Thus, unlike Denisovan molars, which display archaic characteristics not found in modern humans, the only morphologically informative Denisovan postcranial bone identified to date is suggested here to be plesiomorphic and shared between Denisovans and modern humans.

INTRODUCTION

In 2010, a small fragment of a finger phalanx recovered from the Denisova Cave (Denisova 3) in southern Siberia yielded a mitochondrial and a draft genomic sequence that changed our view of the evolution of the Late Pleistocene hominin lineages in Eurasia (*1*, *2*), revealing a previously unknown archaic human population. The phylogenetic analysis of the Denisova 3 mitogenome yielded a divergence date from the ancestors of *Homo sapiens* and Neanderthals of around 1 million years (Ma) ago (1.3 to 0.7 Ma ago) (*1*, *3*, *4*), i.e., much earlier than the mitogenomes of the Neanderthals from the Late Pleistocene that diverged about 500 thousand years (ka) ago [690 to 350 ka ago; (*3*)] (Fig. 1). The nuclear genome, however, suggests a much more recent common ancestor between European Neanderthals (Vindija) and Denisovans dating to around 400 ka ago [440 to 390 ka ago; (*5*)], characterizing Denisovans as a sister group to Neanderthals (*3*, *5*–*8*) (Fig. 1). Later, traces of an even more archaic human have been identified in the Denisova 3 nuclear genome (*7*), and a mitochondrial sequence related to that of Denisova 3 has been found in a ca. 400,000-year-old specimen from Sima de los Huesos (Spain), the nuclear genome of which is more closely related to Neanderthals than to Denisovans (*3*, *9*). Together, these data suggest that the Denisovan mitogenome was either replaced with that of a more archaic human following an admixture event or represents the mitogenome of the common ancestors of Neanderthals and Denisovans before its replacement in the lineage of the Late Pleistocene Neanderthals (Fig. 1) (*2*–*4*, *9*–*10*). The mitogenome of the late Neanderthals either could result from an introgression (i.e., replacement of the mitogenome following admixture) from early anatomically modern humans (AMHs) early after the separation of the AMH and Neanderthal populations, as proposed in one study (*4*), or could be due to incomplete lineage sorting given the uncertainties in the methods to estimate the dates and the wide confidence intervals of the dates proposed (Fig. 1). Furthermore, the comparison of the Denisova 3 nuclear genome with the genomic sequence of a roughly 100,000-year-old Neanderthal from the Denisova Cave revealed that Denisovans had also experienced gene flow from a Neanderthal population (Fig. 1) (*7*). Recently, a bone fragment, also from the Denisova Cave, has been found, through genomic analysis, to belong to a female individual that was the F1 hybrid of a Neanderthal mother and a Denisovan father (*11*). Her maternal Neanderthal contribution is more closely related to the genome of the 40,000-year-old European Neanderthal from Vindija (*5*) than to that of the ~100,000-year-old Neanderthal from the Denisova Cave. Furthermore, the paternal Denisovan genome of the hybrid appears to bear traces of an ancient Neanderthal admixture (*11*). These data indicate that gene flow between Neanderthals and Denisovans was not a rare occurrence.

Molecular dating methods based on mitochondrial sequences indicate that Denisovans must have inhabited the Altai region for over tens of thousands of years (*12*, *13*). Despite the fact that all Denisovan mitochondrial sequences come from the same archeological site, Denisova Cave, the mitochondrial diversity of Denisovans is higher than that of Neanderthals spanning from Spain to the Caucasus (*12*). As inferred from the high-coverage Denisova 3 genome, the Altai population of Denisovans is characterized by low nuclear genome diversity, consistent with a prolonged small population size (*10*). Neanderthal populations also appeared to have been small, as assessed through the analysis of both the Altai and the Vindija genomes (*5*, *7*). On the basis of the modeling, it has been proposed that despite reduced nuclear diversity of the individual local populations, the overall nuclear diversity of the Neanderthal metapopulation was higher (*8*), although this point remains under discussion as it varies with the modeling methods (*6*, *14*). The extent of the Denisovan metapopulation diversity is still awaiting genomic characterization of remains originating from beyond the Denisova Cave, but the presence of Denisovan ancestry in modern human genomes suggests that there were at least two distinct Denisovan populations (*15*). Indeed, the comparison of the genomic sequence of Denisova 3 with the genomes of present-day humans has revealed interbreeding between Denisovans and early AMHs ancestral to present-day human populations not only in Southeast Asia, above all in Melanesians, but also in mainland East Asia (e.g., *15*–*18*).

[1]Institut Jacques Monod, CNRS, University Paris Diderot, 75013 Paris, France. [2]UMR 5199 PACEA, Université de Bordeaux, 33615 Pessac, France. [3]Department of Anthropology, University of Toronto, Toronto, ON M5S 2S2, Canada. [4]Institute of Archaeology and Ethnography, Russian Academy of Sciences, Novosibirsk RU-630090, Russia. [5]Altai State University, Barnaul RU-656049, Russia. [6]Novosibirsk National Research State University, Novosibirsk RU-630090, Russia.
*These authors contributed equally to this work.
†Corresponding author. Email: eabennett@gmail.com (E.A.B.); isabelle.crevecoeur@u-bordeaux.fr (I.C.); bence.viola@utoronto.ca (B.V.); eva-maria.geigl@ijm.fr (E.-M.G.)

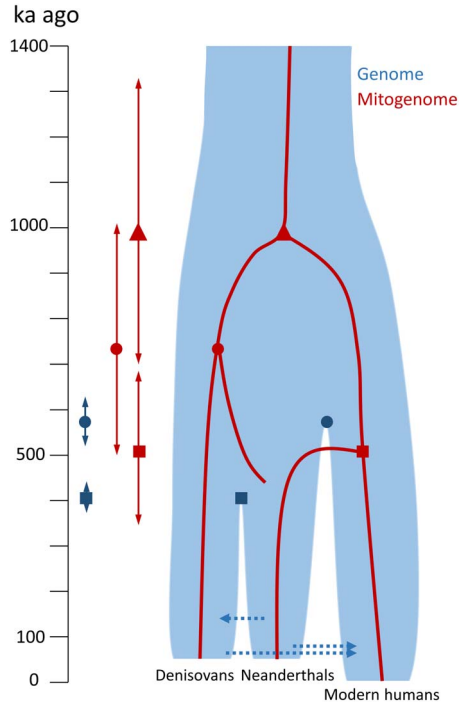

Fig. 1. Model of the phylogeny of Neanderthal, Denisovan, and AMH populations over the past 1,400,000 years as deduced from both nuclear (blue envelope) and mitochondrial genomes (red lines). The vertical axis represents time in thousands of years (ka) ago. Population divergence dates estimated from genomic data and mitochondrial genome bifurcation date estimations originate from Prüfer *et al.* and Meyer *et al.*, respectively (*3*, *5*). Markers on the left indicate the means of the estimates for dates, and error bars indicate 95% confidence intervals. Gene flow events inferred from genome sequences are represented as dotted blue arrows (see text).

The Denisovan ancestry in Melanesians appears to originate from a Denisovan population distantly related to that of the Denisova 3 specimen, and a similar ancestry can also be found in East Asia, particularly in Chinese and Japanese (*15*). In East Asians, a second Denisovan introgression from a Denisovan population more closely related to the Denisova 3 specimen was also detected (*15*). In some cases, the introgression proved to be adaptive, for example, in Tibetans (*19*) and Inuits (*20*).

The distribution and diversity of Denisovan DNA in present-day human populations suggest that Denisovans were once widely distributed throughout Asia (*15*, *18*). This evidence stands in contrast to the scarcity of unambiguously identified remains and of associated characteristic morphological features. What little morphological information that is available comes from a mandible from Xiahe on the Tibetan Plateau and three teeth from the Denisova Cave (*2*, *12*, *13*, *21*). Denisovan mitochondrial genome sequences and low amounts of nuclear DNA have been recovered from a deciduous molar (Denisova 2) and two large-sized permanent molars (Denisova 4 and 8) (*1*, *12*, *13*), while the mandible has been identified as Denisovan based on proteomic information (*21*). The morphology of the Xiahe mandible is similar to that of the Middle Pleistocene specimens, such as the Chinese Lantian and Zhoukoudian, with features of the dental arcade shape that separate it from *Homo erectus* (*21*). It harbors some traits reminiscent of Neanderthals, while other Neanderthal-specific features are lacking (*21*). Thus, the rare Denisovan human remains identified to date show affinity to Middle Pleistocene hominins (*2*, *12*, *13*), particularly to those from China (*21*) and, to a lesser extent, to the Neanderthal lineage (*12*). The permanent molars from the Denisova Cave show complex occlusal morphology (*1*, *12*, *13*). Whether these peculiar characteristics of the molars are the consequence of introgression from a more archaic Eurasian population remains to be seen but cannot be excluded since such a low-level introgression has been identified in the Denisova 3 genome (*7*).

Despite the importance of the Denisovan population for the study of human evolution, identification of Denisovan postcranial remains relies presently only on genomic data, since these remains of Denisovans exhibiting diagnostic features have yet to be reported. Progress in the identification of Denisovan skeletal remains would be instrumental for our understanding of this human lineage, for the identification of Denisovan remains, and for our ability to better characterize Denisovan population genomic diversity. Here, we report the morphometric analysis of a phalanx fragment that we show through its mitochondrial sequence to be the larger distal part of the original Denisova 3 phalanx, the genome of which had been published in 2010 and 2012 (*1*, *2*, *10*). In 2009, the phalanx was cut into two parts. The pictures of the phalanx taken by the Russian scientific team prior to its cutting, however, have been lost. The smaller proximal part of the bone was sent to the Max Planck Institute (MPI) for Evolutionary Anthropology in Leipzig, Germany, and sampling for paleogenomic analysis was performed. The larger distal part was sent to the University of Berkeley, CA, USA, and, in 2010, from there to the "Institut Jacques Monod" (IJM) in Paris, France, where it was measured and photographed and analyzed genetically. It was then returned to the University of Berkeley in 2011.

The present analysis of both phalanx parts represents the first morphological study of nondental remains of this mysterious population that has inhabited Asia for hundreds of thousands of years, has interbred sometimes with Neanderthals and possibly with more archaic Eurasian humans, and continues to endure in the genomes of some present-day human populations.

RESULTS AND DISCUSSION

Complete mitogenome sequence of the Denisova 3 fifth distal manual phalanx allows unambiguous matching of the two parts of the Denisovan phalanx

The Denisova 3 phalanx (2008 Д-2/ 91) was identified in 2008 in layer 11.2 of the East Gallery, square D2, of the Denisova Cave, the date of which is assumed to be more than 50 ka ago (*1*, *2*). To unambiguously match this distal phalanx fragment to the previously described proximal fragment, we retrieved its complete mitogenome [mitochondrial DNA (mtDNA)] sequence using DNA extraction and sequence capture procedures previously described (*22*–*24*). In total, 5838 unique reads were recovered, yielding a 26.7-fold coverage of the mitochondrial genome, of which each base was covered a minimum of twice (42 bases at twofold coverage) and a maximum of 70 times. The resulting consensus was identical to the previously published sequence (*1*) and represents the first replication of the Denisova mtDNA sequence outside of the MPI for Evolutionary Anthropology. This analysis also identified the previously proposed variable length in vivo of the polycytosine run at rCRS (revised Cambridge Reference Sequence) position 5889 (*1*), here found to be between 9 and 14 residues in length. This sequence identity indicates that the two phalanx fragments belong to the same individual.

The exceptional preservation of endogenous DNA in the Denisovan phalanx is evident not only in its high endogenous DNA content but

also in the length of the DNA fragments recovered. While an endogenous DNA content of 70% was recovered from the proximal fragment using the more sensitive single-stranded DNA library preparation method (*10*, *22*), shotgun sequencing of the distal fragment analyzed in this study prepared using a double-stranded library method contained 11.3% endogenous content. This is in line with the ~6-fold increase in endogenous content reported between these two methods (*10*, *22*). Previous analyses of the distribution of the endogenous DNA fragment lengths were performed using only merged reads, which prohibits the identification of endogenous molecules longer than 134 nucleotides. The paired-end mapping strategy used in this study reveals a more complete endogenous fragment length distribution. We show all Denisova-mapping DNA fragments to have a mean distribution of 86.7 base pairs (bp), with a median of 81.3 (Fig. 2). The mean value is similar to that first reported [mean, 85.3 bp; (*1*)], although these two means are skewed toward larger fragments since the library construction method used for these two studies did not recover the greater part of shorter fragments found in libraries prepared with the single-stranded library method (*10*). The longest fragment containing diagnostic Denisovan nucleotide sites recovered in this study was 236 bp.

In contrast to the analyses of the proximal half of the phalanx, which reported low levels of modern human DNA contamination (0.35%) (*1*), the distal half showed the presence of a much higher modern human mitochondrial contaminant (12.1% detected by a similar method). Further investigation revealed that this contaminant could be attributed to a single haplogroup, J1b1a1. Since no member of the IJM laboratory in Paris where the genetic analysis was performed carried mitochondrial haplogroup J, we suspect this contamination to have occurred at some point during the previous handling of the sample, prior to its preparation for genetic analysis.

Anatomical description

When the mitogenome analysis of the proximal epiphysis from the metaphyseal surface indicated that the specimen was not a recent modern human, it was digitized through microcomputed tomography (μCT) at the Department of Human Evolution at the MPI for Evolutionary Anthropology, Leipzig (courtesy of H. Temming and J.-J. Hublin). The reconstructed image based on these scans is shown in Fig. 3. Further sampling for nuclear DNA analysis was performed on this specimen (*2*), and two small holes on the articular surface witness the drilling procedure. The proximal fragment of the phalanx is now composed of two pieces (the proximal epiphysis and the remains of the dorsal part of the diaphysis) (Fig. 3).

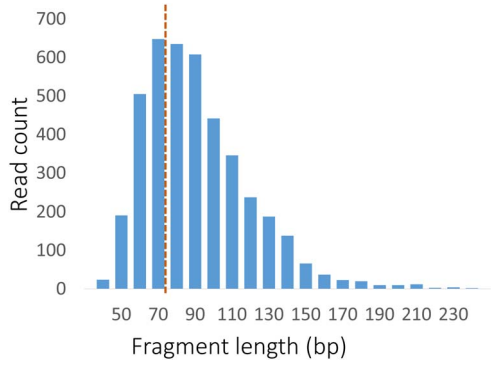

Fig. 2. Distribution of DNA fragment lengths mapping to the Denisova mitochondrial sequence. Fragment lengths given in 10-bp bins are shown. Median is indicated by the dotted orange line. Read pairs that did not overlap sufficiently to be merged (i.e., longer than 134 nucleotides) but that could be mapped as paired-end reads were analyzed individually, and fragments carrying Denisovan single nucleotide polymorphisms (SNPs) were kept.

The larger distal part of the Denisova 3 phalanx was documented in Paris by measurements with a high-precision vernier caliper (Table 1) and high-resolution images under a stereomicroscope (Leica MZ FLIII, PLANAPO 0.63×) prior to sampling (Fig. 3, A, B, and D). The reconstituted image of the entire phalanx is shown in Fig. 3 (A and B) as a virtual reconstruction in the dorsal (Fig. 3A) and palmar (Fig. 3B) views of the distal and proximal part of the phalanx, combining the photographs of the distal part and the three-dimensional (3D) model of the proximal parts. Lateral views of the distal part and several additional views of the proximal part are also shown (Fig. 3D).

Measurements on the original and the rectified stereomicroscope images (Table 1) yielded identical values within ±0.1 mm for the distal and midshaft widths, showing that the pictures are accurate representations of the original bone and could be used for the purpose of a virtual reconstruction. In the original description by Reich *et al.* (*2*), the Denisova 3 phalanx is identified as "the proximal epiphysis of a juvenile manual phalanx, preserving the proximal articular surface and the bone surrounding it." It was proposed that this distal phalanx belonged to an immature individual, probably of an age at death of at least 6 to 7 years but before the start of epiphyseal fusion. The phalanx was not determined with regard to side or ray.

Here, we reanalyzed the μCT scans and photographs of the proximal fragments (the articular surface and the semiring representing the dorsal half of the proximal end of the diaphysis), as well as the photographs of the distal fragment in comparison with the distal phalanges (DPs) of Neanderthals and of Pleistocene and recent modern humans at various stages of development (table S1; see below). The distal border on this surface shows traces of the sawing of the phalanx into two pieces, consistent with those observed on the distal fragment and the proximal semiring fragment of the diaphysis. We draw the conclusion that the morphology of Denisova 3 is incompatible with an unfused immature distal phalanx. First, the palmar surface of the apical tuft is characterized by a well-defined ungual tuberosity, as is the proximal V-shaped ridge of the tuft for the insertion of the flexor digitorum profundus tendon sheath (Fig. 3B). Second, the proximal articular surface fragment on the palmar surface exhibits a relief in the middle part that is unlike the morphology of an unfused proximal epiphysis (Fig. 3B). Last, the μCT images confirm that the distal part on the palmar surface of the articular fragment is a piece of the diaphysis that is fusing (Fig. 3C, red arrows), not the original border of the proximal epiphysis.

Both the semiannular dorsal surface of the diaphysis and the dorsal part of the proximal articular fragment present rounded borders that are consistent with the epiphysis fusing at the time of death (Fig. 3A). Since it takes between 2 and 4 months for an epiphysis to complete the process of fusion, once started, we conclude that the dimensions of the phalanx are close to its final mature state (*25*).

In summary, the evidence from both the distal and proximal fragments indicates that the Denisova 3 DP5 (fifth distal phalanx) belonged to an adolescent. Nuclear DNA analyses show that this individual was a female, allowing us to narrow the age at death around 13.5 years based on the standards from extant humans and assuming that Denisovans had a fairly similar development. If we accept that the phalanx is close to the mature state, then it is possible to tentatively identify both digit and side for Denisova 3. Considering extant modern human diversity, the estimated maximum length of Denisova 3 falls best within the variability

of the DP5s (*25*). In addition, the asymmetry of the ungual tuberosity and the curvature of the shaft in the dorsal view indicate that this DP5 is likely from the right side [(*26*); I. Crevecoeur, personal observation].

Morphometric comparison

We performed morphometric analyses of the DP5 of Denisova 3 based on the measurements taken on the original specimen and the virtual reconstruction for the maximum length (see Fig. 4A for a schematic representation of the various measurements considered here). Using univariate and multivariate analyses, we compared these measurements with data from published and unpublished DPs of Neanderthals, Pleistocene modern humans, and three samples of recent modern humans from France and Belgium dated from the Neolithic to the Middle Ages (table S1; see Fig. 4B for a direct side-by-side comparison of a DP5 from a Neanderthal, a Denisovan, and an AMH). The dimensions of Denisova 3 and the means and SDs of the comparative samples are given in Table 2. The comparison sample includes one AMH and one Neanderthal specimen in which the proximal epiphyses were in the process of fusing.

With the possible exception of the proximal breadth, all dimensions of Denisova 3 fall within the range of variation of modern human DP5s (Fig. 4C). The dimensions of the proximal extremity fall in the lower part of the modern human DP5 variation and outside that of the Neanderthals with regard to the articular surface measurements. This may be related to the state of preservation of the proximal extremity and, probably, also to its state of fusion. While the midshaft height of the diaphysis and the distal height of the apical tuft are close to the modern human mean, the remaining measurements fall into the lower range of the variation, indicating that the Denisova 3 phalanx is gracile. Nevertheless, the fact that we are dealing with an adolescent female must be taken into consideration with regard to potential size and gracility.

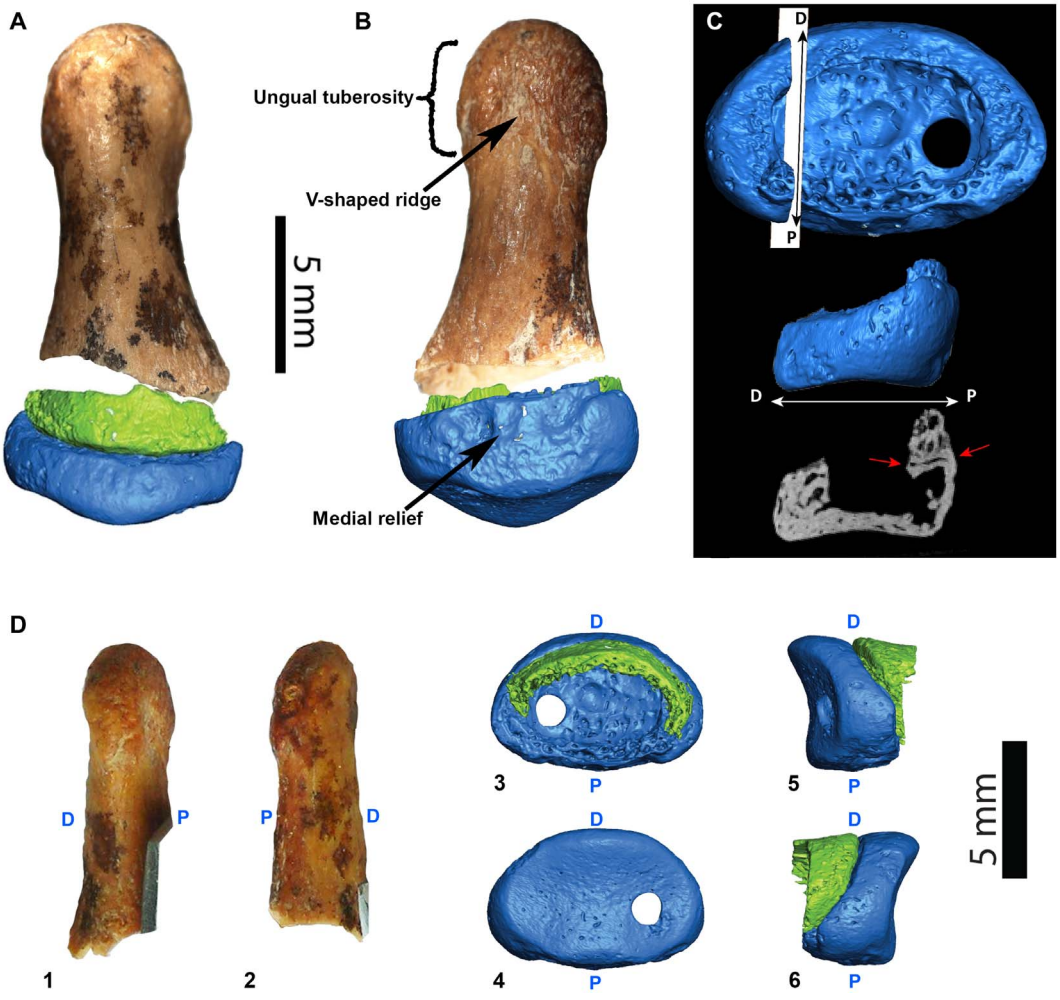

Fig. 3. Views of the Denisova 3 DP5. (**A**) Virtual reconstruction of the Denisova 3 DP5 in dorsal view. Three fragments of the Denisova 3 DP5 are shown. Natural color: Photograph of the distal two-thirds of the phalanx; green: semiring of the dorsal surface of the proximal extremity of the diaphysis of the reconstituted image based on the μCT scan; blue: its proximal articular surface. (**B**) Virtual reconstruction based on the μCT scan of the Denisova 3 DP5 in palmar view. (**C**) Virtual reconstruction of the proximal articular fragment in distal (top) and lateral (middle) views, and the dorsopalmar μCT section of this piece at the level of the fusion (bottom). The D-P line (D, dorsal; P, palmar) represents the location of the section on the distal view and helps to orient the bone in the lateral view. The red arrows indicate the fusing zone. (**D**) Additional views of the distal fragment and the virtual reconstruction of the proximal part of the Denisova phalanx. 1 and 2: Lateral views of the distal fragment; 3: distal; 4: proximal; 5 and 6: lateral views of the proximal fragment. The gray surfaces on the outer border of the phalanx correspond to the forceps with which the phalanx was held while the photo was taken. Photos of the distal part of the phalanx were taken by E.-M.G., IJM, CNRS, Université de Paris, UMR 7592, Paris, France. The renderings of the μCT scans and the virtual reconstruction were performed by B.V., Department of Anthropology, University of Toronto, Toronto, Canada.

Table 1. Measurements of the distal part of the DP5 of Denisova 3. Measurements (in mm) of the distal part of the Denisova 3 phalanx [Denisova Cave 2008/East Gallery/layer 11.2/square D2 Phalanx *tertia* (probably V)] were taken with a vernier caliper directly on the bone fragment and on rectified photographs where applicable.

Measurement	With caliper on distal part (mm)	On rectified photographs (mm)	Comments
Midshaft breadth	3.60	3.7	
Proximal breadth	5.62		? Cut basis
Distal breadth	4.52	4.65	
Maximum length	11.28		Basis cut in a nonperpendicular way
Distal height	2.80		
Midshaft height	3.60		(Difficult since there is no "promontory" above which the measurement should be taken; here: maximal width)

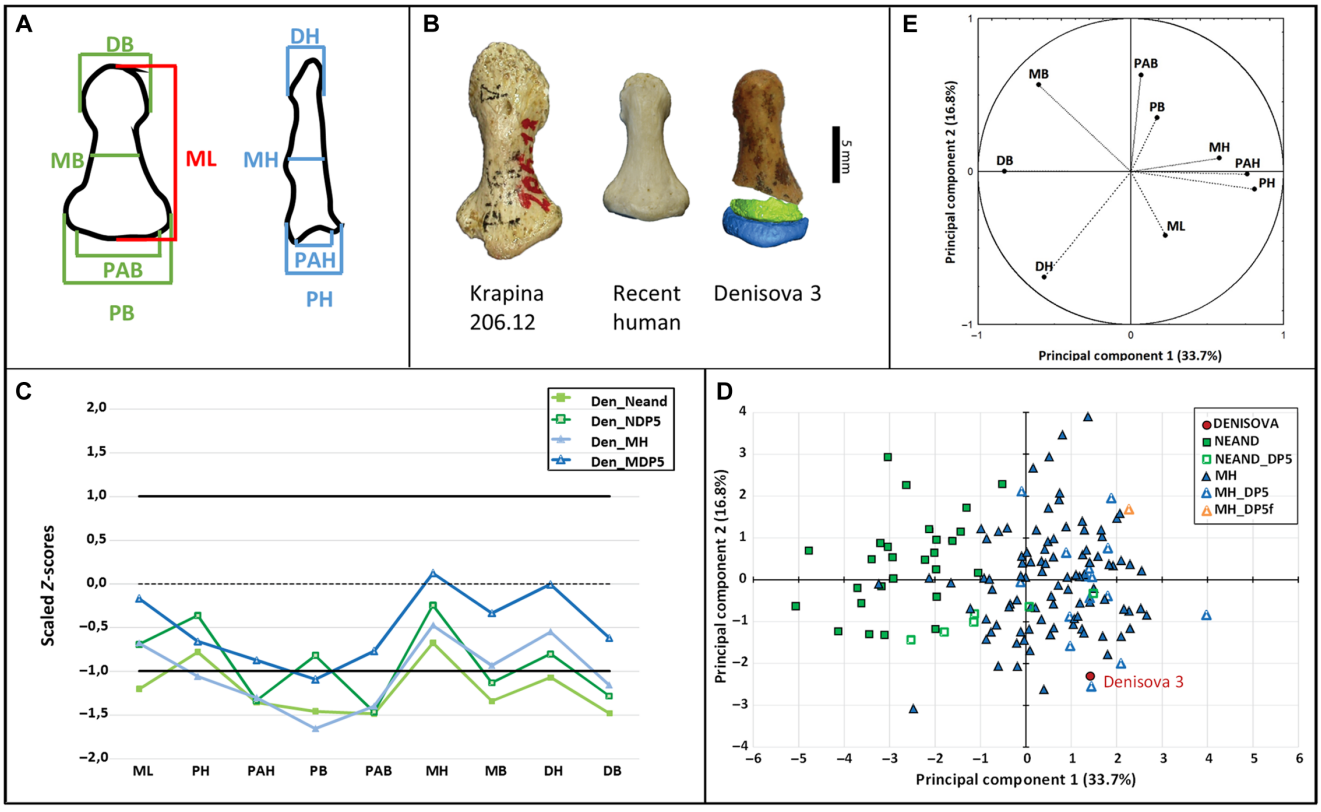

Fig. 4. Measurements of the Denisovan fifth finger phalanx and comparison with those of Neanderthals and AMHs. (**A**) Schematic representation of the various measurements of digital phalanges reported in Table 2 and here: ML, maximal length; PH, proximal height; PAH, proximal articular height; PB, proximal breadth; PAB, proximal articular breadth; MH, midshaft height; MB, midshaft breadth; DB, distal breadth; DH, distal height. (**B**) Comparison of the dorsal view of the DP5 of a Neanderthal (Krapina 206.12), a recent modern human, and the reconstructed Denisova 3. (**C**) Scaled *Z*-scores of the Denisova 3 dimensions (Den) compared to both Neanderthal (NEAND) and pooled modern human (MH) ranges of variation. Den_Neand, Den_RMH, Den_NDP5, and Den_MDP5 indicate the comparison of the values of Denisova's DP5 with the mean and SD of each comparative group from Table 2: NEAND_DP and MH_DP, all distal phalanges; NDP5 and MDP5, DP5s only. *Z*-scores were scaled in a way that zero represents the mean of each range of variation, and +1/−1 represent the upper and lower 95% limits of each range of variation, respectively (see Materials and Methods). Therefore, when a value is lower than −1, it means that it falls outside the lower statistical limit ($P = 0.05$) of the range of variation of the comparative group in question. (**D**) Bivariate plot of the two first principal components of the PCA on size-adjusted measurements of the DPs. MH_DP, pooled sample of Pleistocene and recent modern human DPs; NEAND_DP, Neanderthal DPs. MH-DP5f, fusing DP5 from the modern human sample. (**E**) Correlation circle between the measurements of the distal phalanx and the two first principal components of the PCA on size-adjusted measurements of the DPs shown in (D). Photos of the distal part of the phalanx were taken by E.-M.G., IJM, CNRS, Université de Paris, UMR 7592, Paris, France. The renderings of the µCT scans and the virtual reconstruction were performed by B.V., Department of Anthropology, University of Toronto, Toronto, Canada. Photos of the Krapina 206.12 specimen from the Croatian Natural History Museum collections, Zagreb, Croatia, and from the recent human specimen from the collections of UMR 5199 PACEA, Université de Bordeaux, France, were taken by I.C., UMR 5199 PACEA, Université de Bordeaux, France.

Table 2. Comparison of measurements of the DP5 of Denisova 3 with those of Neanderthals and Pleistocene and recent AMHs. Measurements of the Denisova 3 DP5 (DEN 3_DP5; in mm) based on (i) the images taken under a stereomicroscope for PH, PAH, PAB, MH, DH, and DB; (ii) the 2D reconstruction shown in Fig. 3 for ML; and (iii) the 3D virtual reconstruction for PB, and compared with the means and ranges of the comparative samples. ML, maximal length; PH, proximal height; PAH, proximal articular height; PB, proximal breadth; PAB, proximal articular breadth; MH, midshaft height; MB, midshaft breadth; DB, distal breadth; DH, distal height; m, mean; s, SD; *n*, number; +95, upper limit of 95% of the estimated population based on the sample size; −95, lower limit of 95% of the estimated population based on the sample size. MH_DP, value for the pooled sample of Pleistocene and recent AMH distal phalanges; NEAND_DP, value for the Neanderthal sample of distal phalanges; DP5s, fifth distal phalanges only.

		ML	PH	PAH	PB	PAB	MH	MB	DH	DB
DEN 3–DP5		15.94	5.00	3.73	7.00	6.36	3.34	3.60	2.80	4.52
	m	20.35	6.75	5.64	11.61	10.03	4.07	6.27	4.21	9.57
	s	1.81	1.11	0.69	1.56	1.21	0.53	0.99	0.65	1.9
NEAND_DP	*n*	53	58	52	58	47	60	60	47	61
	+95	19.14	6.80	5.47	11.03	9.26	4.02	5.23	3.5	7.65
	−95	16.71	4.52	4.25	8.49	7.59	3.01	4.29	2.9	5.77
	m	19.07	5.79	4.97	9.89	8.58	3.50	4.90	3.56	7.44
	s	1.90	0.93	0.39	1.51	0.64	0.28	0.49	0.39	0.99
NEAND_DP5	*n*	10	11	10	11	10	11	11	9	12
	+95	23.36	7.86	5.85	13.25	10.03	4.12	5.99	4.46	9.62
	−95	14.77	3.72	4.09	6.52	7.13	2.88	3.81	2.66	5.26
	m	18.20	6.47	5.39	10.48	8.59	3.81	5.01	3.38	6.95
	s	1.68	0.70	0.64	1.06	0.80	0.50	0.76	0.53	1.06
MH_DP	*n*	122	133	129	133	130	134	134	115	134
	+95	21.52	7.85	6.66	12.58	10.17	4.8	6.51	4.43	9.05
	−95	14.87	5.09	4.12	8.38	7.01	2.82	3.51	2.33	4.85
	m	16.41	5.73	4.55	9.13	7.64	3.24	4.02	2.80	5.74
	s	1.29	0.50	0.43	0.89	0.76	0.37	0.57	0.33	0.90
MH_DP5	*n*	17	15	15	16	16	17	17	16	17
	+95	19.14	6.80	5.47	11.03	9.26	4.02	5.23	3.5	7.65
	−95	13.67	4.66	3.63	7.23	6.02	2.46	2.81	2.1	3.83

We performed a multivariate analysis using size-adjusted dimensions to allow a comparison of the DPs based on shape rather than size. The projections along the two first principal components are given in the two following bivariate plots. The scatterplot of the individuals is illustrated in Fig. 4D, and the correlation circle for the original variables in Fig. 4E. The first two principal components represent more than 50% of the total variation. A clear distinction is visible between the Neanderthal and the modern human samples, with Denisova 3 positioned in the lower right quadrant within the modern human variation (Fig. 4D). As expressed by the correlation circle, the Denisovan DP5 differs from that of the Neanderthals in that the former combines a narrow apical tuft (distal breadth) with a thicker DP, particularly at the midshaft and proximal end (midshaft height and proximal height) (Fig. 4E).

Neanderthal DPs have been usually described as notably different from modern humans because of their length and the shape and dimensions of their apical tufts [e.g., (*27*, *28*)]. Neanderthal DPs are proportionally longer with wider extremities compared with modern humans, which gives the impression of flattening of the bone (*29*). This conformation of the apical tuft among Neanderthals seems to be related to functional rather than cold climate adaptations (*30*).

These characteristics are confirmed by our analysis, but additional observations can be made regarding the DP5s. Neanderthal DP5s seem to occupy a specific position compared with the other Neanderthal DPs. This difference between the fifth and the other phalanges that is not visible in the modern human sample is due to both the specific morphology of the Neanderthal DP5 compared with the other digits, driven by the shape of the midshaft and the apical tuft, which are both narrower than the remaining digits. On the contrary, when not taking into account the size factor, AMH DP5s scatter within the variability of the other DPs.

The nuclear genomes of Neanderthals and Denisovans are closer to each other than to modern humans, and it has been estimated that the population split time between Denisovans and Neanderthals is about 410 ka ago (*5*), whereas the population split time between these archaic humans and the ancestors of AMHs is about 580 ka ago (Fig. 1) (*5*, *7*, *10*). Despite being evolutionary sister groups, the Denisova 3 DP5 does not

exhibit any of the features seen in Neanderthals. Its morphology is indistinguishable from that of modern humans and located within modern human variation, which likely represents the plesiomorphic morphology of nonpollical DPs within the genus *Homo* as seen in both the Olduvai Hominin OH 7 and the Dmanisi hominins (*31*, *32*). This suggests that the Neanderthal-specific characters of the phalanx evolved after the divergence of Denisovans and Neanderthals. The only Neanderthal DP5 that falls in the middle of the modern human variation is from Moula-Guercy, one of the earliest members of the Neanderthal lineage from our sample dating to around 100 ka ago (*33*). This observation raises the possibility that the derived properties of the Neanderthal phalanx occurred rather late during the evolution of the Neanderthals. The similarity between the Denisovan phalanx and those of AMHs contrasts with the morphology of the molars of the Denisova individuals that are morphologically closer to more archaic humans from the Middle Pleistocene to the Late Pleistocene (*2*, *12*, *13*).

CONCLUSIONS

We could genetically link the distal part of a DP5 from the Denisova Cave in Siberia to the Denisova 3 phalanx fragment, whose genome identified it as a representative of a population more closely related to Neanderthals than to modern humans. Morphometric analysis based on high-resolution pictures, linear measurements, and the comparison with the DP5s of Neanderthals as well as Pleistocene and recent modern humans shows that it is within the range of variation of the dimensions of the DP5s of modern humans and distinct from that of Neanderthals. We propose that this represents the plesiomorphic morphology within the genus *Homo* (*32*), consistent with the morphology of early *Homo* DPs (*31*, *32*), and that the derived morphology of the Neanderthal phalanx evolved after their split from the ancestors of the young woman from the Denisova Cave (see Fig. 1). This finding calls for caution when identifying potential Denisovan postcranial skeletal remains beyond Denisova, as their morphology might be ambiguous or more similar to modern humans than to Neanderthals.

MATERIALS AND METHODS

Recovery of the phalanx

In 2009, the phalanx was cut into two parts. Unfortunately, the pictures of the phalanx taken by the Russian scientific team prior to its cutting have been lost. The smaller proximal part of the bone was sent to the MPI for Evolutionary Anthropology in Leipzig, Germany, and sampling for paleogenomic analysis was performed by drilling into the proximal epiphysis from the metaphyseal surface. The larger distal part was sent to the University of Berkeley, CA, USA, and, in 2010, from there to the IJM in Paris, France, where it was measured and photographed, and a thin portion, removed from the proximal end of the distal part of the phalanx, was analyzed genetically. It was then returned to the University of Berkeley in 2011.

Determination of the age of the individual

According to Scheuer and Black (*25*), when fusing, the palmar border of the proximal epiphysis develops a medial and lateral tongue of bone that grows upward toward the diaphysis. The dorsal surface responds differently by forming a sloping distal metaphyseal surface, which is convex dorsopalmarly. The fusion of the distal phalangeal epiphysis occurs at the age between 13.6 and 16 years, depending on the sex (*34*). Since both the semiannular dorsal surface of the diaphysis and the dorsal part of the proximal articular fragment present rounded borders that are consistent with the epiphysis fusing at the time of death (Fig. 3A) and since it takes between 2 and 4 months for an epiphysis to complete the process of fusion, once started, we concluded that the dimensions of the phalanx are close to its final mature state (*25*).

Measurements of the phalanx

The larger distal part of the Denisova 3 phalanx had been measured with a high-precision vernier caliper (0 to 200 mm; Graduation 0.02 mm, DIN862) prior to sampling for DNA analysis (see Table 1). Then, images were taken under a stereomicroscope (Leica MZ FLIII, PLANAPO 0.63×) on a graph paper background. These images were rectified using the graph paper as a perspective reference and scale in Adobe Photoshop CC (Perspective tool, Adobe Inc. 2018).

Morphometric analyses

For the morphometric comparative analysis, DPs from published and unpublished Neanderthals, Pleistocene modern humans, and three samples of recent modern humans from France and Belgium dated from the Neolithic to the Middle Ages (including a modern human and a Neanderthal DP5 undergoing epiphyseal fusion) were assigned to a specific digit based on their respective length and robustness [DP3 ≥ DP4 > DP2 > DP5; (*25*)] and the morphology of their extremities (table S1) (*26*, *27*, *35*). When uncertain, the DPs were pooled in two additional ranks: DP2–4 or DP2–5. The measurements used were those defined by Musgrave (*36*) for phalanges. The dimensions of Denisova 3 used were those taken on the original specimen for all measurements except the maximum length, which was taken on the virtual reconstruction of the two fragments (Table 2).

We used univariate and multivariate analyses to explore the morphometric characteristics of the DP5 Denisova 3. To compare the dimensions of Denisova 3 to the means and SDs of the Neanderthal and modern human comparative groups, we calculated the scaled *Z*-score with the distribution variance estimated by the sample variance. The scaled *Z*-score was chosen such that at $Z = 1$, it will correspond to a 5% *P* value for two tails. This was achieved by introducing a scaling factor for the *Z*-score, which effectively uses a normal distribution with zero mean and variance 1/1.9599. The scaled *Z*-score was estimated modeling a student's distribution and correcting for sample size using the following formula (*37*, *38*)

$$Z^* = \frac{|X - m|}{t_{0.975;n-1} * \sqrt{s^2\left(1 + \frac{1}{n}\right)}}$$

where Z^* is the scaled *Z*-score, X is the Denisova 3 measurement, m is the mean of the corresponding measurement in the Neanderthal or AMH population, s is the SD, and n is the sample size. Last, $t_{0.975;n-1}$ is the 97.5% unilateral quantile of the Student's distribution for $n - 1$ degree of freedom. The multivariate analysis of the various DPs was performed using principal components analyses (PCAs) on dimensions that were size adjusted through the normalization of each dimension by the geometric mean of all dimensions (*39*, *40*).

DNA extraction, mitochondrial enrichment, and sequencing

DNA extraction, purification, and library construction were performed in the high-containment ancient DNA laboratory of the IJM in Paris (see the Supplementary Materials). Bone powder (39 mg) was scraped with a sterile scalpel from the proximal surface, which had been cut

prior to its arrival at the IJM. It was then incubated in 1.5 ml of 0.5 M EDTA, 0.25 M PO_4^{3-} (pH 8.0), and 1% β-mercaptoethanol extraction solution and placed on a rotating mixer for 22 hours at 37°C. DNA was purified with a silica membrane spin column (QIAquick Gel Extraction kit, Qiagen, Hilden, Germany) using a modified QIAquick protocol that increases the ratio of guanidine thiocyanate and isopropanol to sample volume [modified from (*23*); see the Supplementary Materials]. After treating with USER enzyme mix to eliminate cytosine deaminated bases, double-stranded libraries were prepared from 1 μl of purified extract using the NxSeq AmpFREE Low DNA Library Kit (Lucigen, Middleton, WI, USA), but substituting dual-barcoded single-stranded library adapters (*41*) for the indexing primers supplied by Lucigen. Amplified libraries were purified/size selected using NucleoMag beads (Macherey-Nagel) with a volume ratio of beads to libraries of 1:3. They were then enriched for mtDNA with a single round of capture using biotinylated RNA baits generated from human mtDNA (courtesy of L. Cardin and S. Brunel), as previously described (*24*), except that the final elution of captured libraries from the beads was performed with a 5-min incubation step at 95°C in 30 μl of 10 mM Tris-HCl, 0.05% Tween 20, followed by the transfer of the supernatant to a clean tube. Enriched libraries were amplified, then purified using NucleoMag beads, and quantified using a NanoDrop ND-1000 spectrophotometer (Thermo Fisher Scientific, Waltham, MA, USA), a Qubit 2.0 Fluorometer (Thermo Fisher Scientific), quantitative polymerase chain reaction (PCR), and a Bioanalyzer (Agilent, Santa Clara, CA, USA). Libraries were then sequenced on an Illumina MiSeq system using a v3 Reagent Kit for 2 × 76 cycles and substituting the custom CL72 primer for read 1 as described (*41*). A more detailed description is available in the Supplementary Materials and Methods.

Sequence analysis

Adapters were trimmed, sequences were merged, and reads shorter than 28 bp were discarded. Unmerged reads were kept apart and processed in parallel. All reads were then aligned to the Denisova mitochondrial genome sequence (*1*) using BWA aln (*42*), followed by either samse (merged reads) or sampe (nonmerged reads), and duplicate reads were removed. The two resulting bam files were then merged into a single file, and a consensus sequence was constructed.

The level of contaminating modern human DNA was measured by aligning the reads to a multi-fasta reference sequence containing both the Denisova and modern human rCRS mitochondrial sequences, removing PCR duplicates, and counting reads and bases overlapping any of the 182 sites where the Denisovan mitochondrial sequence is different from a panel of modern humans. This resulted in 12.1% bases and 13.9% reads originating from modern human mitochondria. A consensus modern human contaminating sequence covering 89% of bases was generated from reads mapping to the human rCRS rather than to the Denisovan sequence, and haplogroup assignment was assessed both by using the K-mer–based haplogroup assignment software Phy-Mer (*43*) and by its position on a maximum likelihood tree of reference haplogroups. A more detailed description is available in the Supplementary Materials and Methods.

SUPPLEMENTARY MATERIALS

Supplementary material for this article is available at http://advances.sciencemag.org/cgi/content/full/5/9/eaaw3950/DC1

Supplementary Materials and Methods

Table S1. Composition of the comparative samples of DPs.

References (*44*–*57*)

REFERENCES AND NOTES

1. J. Krause, Q. Fu, J. M. Good, B. Viola, M. V. Shunkov, A. P. Derevianko, S. Pääbo, The complete mitochondrial DNA genome of an unknown hominin from southern Siberia. *Nature* **464**, 894–897 (2010).
2. D. Reich, R. E. Green, M. Kircher, J. Krause, N. Patterson, E. Y. Durand, B. Viola, A. W. Briggs, U. Stenzel, P. L. F. Johnson, T. Maricic, J. M. Good, T. Marques-Bonet, C. Alkan, Q. Fu, S. Mallick, H. Li, M. Meyer, E. E. Eichler, M. Stoneking, M. Richards, S. Talamo, M. V. Shunkov, A. P. Derevianko, J. J. Hublin, J. Kelso, M. Slatkin, S. Pääbo, Genetic history of an archaic hominin group from Denisova Cave in Siberia. *Nature* **468**, 1053–1060 (2010).
3. M. Meyer, Q. Fu, A. Aximu-Petri, I. Glocke, B. Nickel, J.-L. Arsuaga, I. Martínez, A. Gracia, J. M. B. de Castro, E. Carbonell, S. Pääbo, A mitochondrial genome sequence of a hominin from Sima de los Huesos. *Nature* **505**, 403–406 (2014).
4. C. Posth, C. Wißing, K. Kitagawa, L. Pagani, L. van Holstein, F. Racimo, K. Wehrberger, N. J. Conard, C. J. Kind, H. Bocherens, J. Krause, Deeply divergent archaic mitochondrial genome provides lower time boundary for African gene flow into Neanderthals. *Nat. Commun.* **8**, 16046 (2017).
5. K. Prüfer, C. de Filippo, S. Grote, F. Mafessoni, P. Korlević, M. Hajdinjak, B. Vernot, L. Skov, P. Hsieh, S. Peyrégne, D. Reher, C. Hopfe, S. Nagel, T. Maricic, Q. Fu, C. Theunert, R. Rogers, P. Skoglund, M. Chintalapati, M. Dannemann, B. J. Nelson, F. M. Key, P. Rudan, Ž. Kućan, I. Gušić, L. V. Golovanova, V. B. Doronichev, N. Patterson, D. Reich, E. E. Eichler, M. Slatkin, M. H. Schierup, A. M. Andrés, J. Kelso, M. Meyer, S. Pääbo, A high-coverage Neandertal genome from Vindija Cave in Croatia. *Science* **358**, 655–658 (2017).
6. F. Mafessoni, K. Prüfer, Better support for a small effective population size of Neandertals and a long shared history of Neandertals and Denisovans. *Proc. Natl. Acad. Sci. U.S.A.* **114**, E10256–E10257 (2017).
7. K. Prüfer, F. Racimo, N. Patterson, F. Jay, S. Sankararaman, S. Sawyer, A. Heinze, G. Renaud, P. H. Sudmant, C. de Filippo, H. Li, S. Mallick, M. Dannemann, Q. Fu, M. Kircher, M. Kuhlwilm, M. Lachmann, M. Meyer, M. Ongyerth, M. Siebauer, C. Theunert, A. Tandon, P. Moorjani, J. Pickrell, J. C. Mullikin, S. H. Vohr, R. E. Green, I. Hellmann, P. L. F. Johnson, H. Blanche, H. Cann, J. O. Kitzman, J. Shendure, E. E. Eichler, E. S. Lein, T. E. Bakken, L. V. Golovanova, V. B. Doronichev, M. V. Shunkov, A. P. Derevianko, B. Viola, M. Slatkin, D. Reich, J. Kelso, S. Pääbo, The complete genome sequence of a Neanderthal from the Altai Mountains. *Nature* **505**, 43–49 (2014).
8. A. R. Rogers, R. J. Bohlender, C. D. Huff, Early history of Neanderthals and Denisovans. *Proc. Natl. Acad. Sci. U.S.A.* **114**, 9859–9863 (2017).
9. M. Meyer, J.-L. Arsuaga, C. de Filippo, S. Nagel, A. Aximu-Petri, B. Nickel, I. Martínez, A. Gracia, J. M. B. de Castro, E. Carbonell, B. Viola, J. Kelso, K. Prüfer, S. Pääbo, Nuclear DNA sequences from the Middle Pleistocene Sima de los Huesos hominins. *Nature* **531**, 504–507 (2016).
10. M. Meyer, M. Kircher, M.-T. Gansauge, H. Li, F. Racimo, S. Mallick, J. G. Schraiber, F. Jay, K. Prufer, C. de Filippo, P. H. Sudmant, C. Alkan, Q. Fu, R. Do, N. Rohland, A. Tandon, M. Siebauer, R. E. Green, K. Bryc, A. W. Briggs, U. Stenzel, J. Dabney, J. Shendure, J. Kitzman, M. F. Hammer, M. V. Shunkov, A. P. Derevianko, N. Patterson, A. M. Andres, E. E. Eichler, M. Slatkin, D. Reich, J. Kelso, S. Pääbo, A high-coverage genome sequence from an archaic Denisovan individual. *Science* **338**, 222–226 (2012).
11. V. Slon, F. Mafessoni, B. Vernot, C. de Filippo, S. Grote, B. Viola, M. Hajdinjak, S. Peyrégne, S. Nagel, S. Brown, K. Douka, T. Higham, M. B. Kozlikin, M. V. Shunkov, A. P. Derevianko, J. Kelso, M. Meyer, K. Prüfer, S. Pääbo, The genome of the offspring of a Neanderthal mother and a Denisovan father. *Nature* **561**, 113–116 (2018).
12. S. Sawyer, G. Renaud, B. Viola, J.-J. Hublin, M.-T. Gansauge, M. V. Shunkov, A. P. Derevianko, K. Prüfer, J. Kelso, S. Pääbo, Nuclear and mitochondrial DNA sequences from two Denisovan individuals. *Proc. Natl. Acad. Sci. U.S.A.* **112**, 15696–15700 (2015).
13. V. Slon, B. Viola, G. Renaud, M.-T. Gansauge, S. Benazzi, S. Sawyer, J.-J. Hublin, M. V. Shunkov, A. P. Derevianko, J. Kelso, K. Prüfer, M. Meyer, S. Pääbo, A fourth Denisovan individual. *Sci. Adv.* **3**, e1700186 (2017).
14. A. R. Rogers, R. J. Bohlender, C. D. Huff, Reply to Mafessoni and Prufer: Inferences with and without singleton site patterns. *Proc. Natl. Acad. Sci. U.S.A.* **114**, E10258–E10260 (2017).
15. S. R. Browning, B. L. Browning, Y. Zhou, S. Tucci, J. M. Akey, Analysis of human sequence data reveals two pulses of archaic denisovan admixture. *Cell* **173**, 53–61.e9 (2018).
16. L. Abi-Rached, M. J. Jobin, S. Kulkarni, A. McWhinnie, K. Dalva, L. Gragert, F. Babrzadeh, B. Gharizadeh, M. Luo, F. A. Plummer, J. Kimani, M. Carrington, D. Middleton, R. Rajalingam, M. Beksac, S. G. E. Marsh, M. Maiers, L. A. Guethlein, S. Tavoularis, A.-M. Little, R. E. Green, P. J. Norman, P. Parham, The shaping of modern human immune systems by multiregional admixture with archaic humans. *Science* **334**, 89–94 (2011).
17. F. Racimo, D. Marnetto, E. Huerta-Sanchez, Signatures of archaic adaptive introgression in present-day human populations. *Mol. Biol. Evol.* **34**, 296–317 (2017).

18. B. Vernot, S. Pääbo, The predecessors within. *Cell* **173**, 6–7 (2018).
19. E. Huerta-Sánchez, X. Jin, Asan, Z. Bianba, B. M. Peter, N. Vinckenbosch, Y. Liang, X. Yi, M. He, M. Somel, P. Ni, B. Wang, X. Ou, Huasang, J. Luosang, Z. X. P. Cuo, K. Li, G. Gao, Y. Yin, W. Wang, X. Zhang, X. Xu, H. Yang, Y. Li, J. Wang, J. Wang, R. Nielsen, Altitude adaptation in Tibetans caused by introgression of Denisovan-like DNA. *Nature* **512**, 194–197 (2014).
20. F. Racimo, D. Gokhman, M. Fumagalli, A. Ko, T. Hansen, I. Moltke, A. Albrechtsen, L. Carmel, E. Huerta-Sánchez, R. Nielsen, Archaic adaptive introgression in TBX15/WARS2. *Mol. Biol. Evol.* **34**, 509–524 (2017).
21. F. Chen, F. Welker, C.-C. Shen, S. E. Bailey, I. Bergmann, S. Davis, H. Xia, H. Wang, R. Fischer, S. E. Freidline, T.-L. Yu, M. M. Skinner, S. Stelzer, G. Dong, Q. Fu, G. Dong, J. Wang, D. Zhang, J.-J. Hublin, A late Middle Pleistocene Denisovan mandible from the Tibetan Plateau. *Nature* **569**, 409–412 (2019).
22. E. A. Bennett, D. Massilani, G. Lizzo, J. Daligault, E.-M. Geigl, T. Grange, Library construction for ancient genomics: Single strand or double strand? *Biotechniques* **56**, 289–290, 292-286, 298, passim (2014).
23. O. Gorgé, E. A. Bennett, D. Massilani, J. Daligault, M. Pruvost, E.-M. Geigl, T. Grange, Analysis of ancient DNA in microbial ecology. *Methods Mol. Biol.* **1399**, 289–315 (2016).
24. D. Massilani, S. Guimaraes, J.-P. Brugal, E. A. Bennett, M. Tokarska, R.-M. Arbogast, G. Baryshnikov, G. Boeskorov, J.-C. Castel, S. Davydov, S. Madelaine, O. Putelat, N. N. Spasskaya, H.-P. Uerpmann, T. Grange, E.-M. Geigl, Past climate changes, population dynamics and the origin of Bison in Europe. *BMC Biol.* **14**, 93 (2016).
25. L. Scheuer, S. Black, *Developmental Juvenile Osteology* (Academic Press, San Diego, 2000).
26. D. Case, J. Heilman, New siding techniques for the manual phalanges: A blind test. *Int. J. Osteoarcheol.* **16**, 338–346 (2006).
27. J. H. Musgrave, How dextrous was Neandertal Man? *Nature* **233**, 538–541 (1971).
28. E. Trinkaus, *The Shanidar Neandertals* (Academic Press, New York-London, 1983).
29. W. A. Niewoehner, in *Neanderthals Revisited: New Approaches and Perspectives*, K. Harvati, T. Harrison, Eds. (Springer, Dordrecht, 2006), pp. 157–190.
30. E. S. Mittra, H. F. Smith, P. Lemelin, W. J. Jungers, Comparative morphometrics of the primate apical tuft. *Am. J. Phys. Anthropol.* **134**, 449–459 (2007).
31. R. L. Susman, N. Creel, Functional and morphological affinities of the subadult hand (O.H. 7) from Olduvai Gorge. *Am. J. Phys. Anthropol.* **51**, 311–332 (1979).
32. D. Lordkipanidze, T. Jashashvili, A. Vekua, M. S. P. de León, C. P. E. Zollikofer, G. P. Rightmire, H. Pontzer, R. Ferring, O. Oms, M. Tappen, M. Bukhsianidze, J. Agusti, R. Kahlke, G. Kiladze, B. Martinez-Navarro, A. Mouskhelishvili, M. Nioradze, L. Rook, Postcranial evidence from early Homo from Dmanisi, Georgia. *Nature* **449**, 305–310 (2007).
33. A. Defleur, T. White, P. Valensi, L. Slimak, E. Crégut-Bonnoure, Neanderthal cannibalism at Moula-Guercy, Ardèche, France. *Science* **286**, 128–131 (1999).
34. M. Schaefer, S. Black, L. Scheuer, *Juvenile Osteology. A Laboratory and Field Manual* (Elsevier, Academic Press, Amsterdam, 2009).
35. J. M. F. Landsmeer, Anatomical and functional investigations of the articulations of the human fingers. *Acta Anat. Suppl.* **25**, 1–69 (1955).
36. J. H. Musgrave (University of Cambridge, Cambridge, 1970).
37. B. Maureille, H. Rougier, F. Houët, B. Vandermeersch, Les dents inférieures du Néandertalien Regourdou 1 (commune de Montignac, Dordogne): Analyses métriques et comparatives. *Paleo* **13**, 183–200 (2001).
38. H. Scolan, F. Santos, A.-M. Tillier, B. Maureille, A. Quintard, De nouveaux vestiges néandertaliens à Las Pélénos (Monsempron-Libos, Lot-et-Garonne, France). *Bull. Mém. Soc. Anthropol. Paris* **24**, 69–95 (2012).
39. J. N. Darroch, J. E. Mosimann, Canonical and principal components of shape. *Biometrika* **72**, 241–252 (1985).
40. W. L. Jungers, A. B. Falsetti, C. E. Wall, Shape, relative size, and size-adjustments in morphometrics. *Yearbook Phys. Anthropol.* **38**, 137–161 (1995).
41. M.-T. Gansauge, M. Meyer, Single-stranded DNA library preparation for the sequencing of ancient or damaged DNA. *Nat. Protoc.* **8**, 737–748 (2013).
42. H. Li, R. Durbin, Fast and accurate short read alignment with Burrows-Wheeler transform. *Bioinformatics* **25**, 1754–1760 (2009).
43. D. Navarro-Gomez, J. Leipzig, L. Shen, M. Lott, A. P. M. Stassen, D. C. Wallace, J. L. Wiggs, M. J. Falk, M. van Oven, X. Gai, Phy-Mer: A novel alignment-free and reference-independent mitochondrial haplogroup classifier. *Bioinformatics* **31**, 1310–1312 (2015).
44. S. Champlot, C. Berthelot, M. Pruvost, E. A. Bennett, T. Grange, E.-M. Geigl, An efficient multistrategy DNA decontamination procedure of PCR reagents for hypersensitive PCR applications. *PLOS ONE* **5**, e13042 (2010).
45. A. Peltzer, G. Jäger, A. Herbig, A. Seitz, C. Kniep, J. Krause, K. Nieselt, EAGER: Efficient ancient genome reconstruction. *Genome Biol.* **17**, 60 (2016).
46. H. Suzuki, F. Takai, *The Amud Man and his Cave Site* (Academic Press Japan, Tokyo, 1970).
47. M. D. Garralda, B. Vandermeersch, Les néandertaliens de la grotte de Combe-Grenal (Domme, Dordogne, France) / The Neanderthals from Combe-Grenal cave (Domme, Dordogne, France). *Paléo* **12**, 213–259 (2000).
48. M. B. Mednikova, Distal phalanx of the hand of Homo from Denisova cave stratum 12: A tentative description. *Archaeol. Ethnol. Anthropol. Eurasia* **41**, 146–155 (2013).
49. F. H. Smith, M. Ostendorf Smith, R. W. Schmitz, in *Neanderthal 1856–2006*, R. W. Schmitz, Ed. (Verlag Philipp von Zabern, Mainz am Rhein, 2006), pp. 187–246.
50. B. Vandermeersch, in *Le squelette Moustérien de Kébara 2*, O. Bar-Yosef, B. Vandemeersch, Eds. (Edition du CNRS, Paris, 1991), pp. 157–178.
51. M. J. Walker, J. Gibert, M. V. López, A. V. Lombardi, A. Pérez-Pérez, J. Zapata, J. Ortega, T. Higham, A. Pike, J.-L. Schwenninger, J. Zilhão, E. Trinkaus, Late neandertals in southeastern Iberia: Sima de las Palomas del Cabezo Gordo, Murcia, Spain. *Proc. Natl. Acad. Sci. U.S.A.* **105**, 20631–20636 (2008).
52. M. J. Walker, J. Ortega, M. V. López, K. Parmová, E. Trinkaus, Neandertal postcranial remains from the Sima de las Palomas del Cabezo Gordo, Murcia, Southeastern Spain. *Am. J. Phys. Anthropol.* **144**, 505–515 (2011).
53. B. Mersey, R. S. Jabbour, K. Brudvik, A. Defleur, Neanderthal hand and foot remains from Moula-Guercy, Ardèche, France. *Am. J. Phys. Anthropol.* **152**, 516–529 (2013).
54. V. Sládek, E. Trinkaus, S. W. Hillson, T. W. Holliday, *The People of the Pavlovian. Skeletal Catalogue and Osteometrics of the Gravettian Fossil Hominids from Dolní Věstonice and Pavlov* (Akademie věd Ceske Republicky, Brno, 2000).
55. O. M. Pearson, J. G. Fleagle, F. E. Grine, D. F. Royer, Further new hominin fossils from the Kibish Formation, southwestern Ethiopia. *J. Hum. Evol.* **55**, 444–447 (2008).
56. B. Vandermeersch, *Les hommes fossiles de Qafzeh (Israël)* (Edition du CNRS, 1981).
57. F. E. Grine, R. Klein, Late Pleistocene human remains from the Sea Harvest Site, Saldanha Bay, South Africa. *Suid-AfrilcaanseTydskrifvir Wetenskap* **89**, 145–152 (1993).

Acknowledgments: We are grateful to the following curators and scientists who granted us access to fossil material or helped in acquiring the data: E. Dewaemme, C. Polet, and P. Semal (Royal Belgian Institute of Natural Sciences, Brussels, Belgium); D. Castex and P. Courtaud (Bordeaux University, Pessac, France); J. Radovcic (Croatian Natural History Museum) and the European TNT project for the access to the Krapina collection; A. Froment, D. Grimaud-Hervé, P. Mennecier (National Museum of Natural History, Paris, France), and A. Thomas for the study of La Ferrassie 1, 2, and 3 hand bones; B. Vandermeersch and J.-J. Hublin (Max Planck-Insitute, Leipzig, Germany) for the analysis of the Saint-Césaire 1 remains; V. Merlin Anglade (Musée d'Art et d'Archéologie du Périgord, Périgueux, France) for the access to the Regourdou 1 Neanderthal specimen; K. Kolobova and S. Markin for the access to the Chagyrskaya hand remains; and I. Hershkovitz and J. Abramov (Tel-Aviv University, Israel) for pictures and measurements of Kebara 2 and Amud 1 phalanges. We thank E. Rubin (University Berkeley) for giving us the opportunity to perform the genomic work on the Denisova 3 distal phalanx. We thank two anonymous reviewers for valuable comments that helped us to improve the manuscript. **Funding:** The study was supported by the French National Research Center CNRS. E.A.B. was supported by the CNRS and the Labex "Who am I." B.V. was supported by the Social Sciences and Humanities Research Council of Canada (insight grant 435-2018-0943). The paleogenomic facility obtained support from the University Paris Diderot within the program "Actions de recherches structurantes." The sequencing facility of the IJM, Paris, was supported by grants from the University Paris Diderot, the Fondation pour la Recherche Médicale (DGE20111123014), and the Région Ile-de-France (11015901). The research of I.C. and B.M. was supported by the ANR (French National Research Agency) project LabEx Sciences archéologiques de Bordeaux, no. ANR-10-LABX-52, and the project "NATCH" convention 2016-1R40240-00007349-00007350 of the Région Nouvelle Aquitaine. **Author contributions:** E.-M.G. and B.M. designed the project. E.A.B. and T.G. designed the molecular biology experiments. E.A.B. performed the molecular biology experiments and mtDNA analysis. E.-M.G. measured and photographed the phalanx using a stereomicroscope. I.C. and B.V. measured the phalanx on the stereomicroscope photos. I.C. performed the comparative analysis with support from B.M. B.V. carried out the virtual reconstruction of the phalanx. A.P.D. and M.V.S. directed the excavations. E.-M.G., E.A.B., T.G., and I.C. wrote the manuscript with contributions from B.V. and B.M. **Competing interests:** The authors declare that they have no competing interests. **Data and materials availability:** Ancient DNA sequences are available from the NCBI Sequence Read Archive SRA ID PRJNA525697. All data needed to evaluate the conclusions in the paper are present in the paper and/or the Supplementary Materials. Additional data related to this paper may be requested from the authors.

Submitted 17 December 2018
Accepted 11 July 2019
Published 4 September 2019
10.1126/sciadv.aaw3950

Citation: E. A. Bennett, I. Crevecoeur, B. Viola, A. P. Derevianko, M. V. Shunkov, T. Grange, B. Maureille, E.-M. Geigl, Morphology of the Denisovan phalanx closer to modern humans than to Neanderthals. *Sci. Adv.* **5**, eaaw3950 (2019).